An ab Initio MO Study on Two Possible Stereochemical Reaction Paths for Methanol Dehydrogenation with $Ru(OAc)Cl(PEtPh_2)_3$

Hiroaki Itagaki,*,† Nobuaki Koga,‡ Keiji Morokuma,‡ and Yasukazu Saito†

Department of Industrial Chemistry, Faculty of Engineering, University of Tokyo, Hongo, Bunkyo-ku, Tokyo 113, Japan, and Institute for Molecular Science, Myodaiji, Okazaki 444, Japan

Received November 2, 1992

An ab initio MO study was carried out for two possible stereochemical reaction paths for methanol dehydrogenation with $Ru(OAc)Cl(PEtPh_2)_3$, taking into account the coordination of solvent methanol to reaction intermediates. An appreciable trans influence of the phosphine ligand was indicated from the optimized geometry of $Ru(\eta^2\text{-}OAc)Cl(PH_3)_3$, a model complex of the $Ru(OAc)Cl(PEtPh_2)_3$ catalyst, since the acetato Ru–O bond trans-disposed to phosphine was more weakened than the other. $Ru(\eta^1\text{-}OAc)Cl(MeOH)(PH_3)_3$, an assumed intermediate, was relatively stable at the coordination mode of methanol trans-disposed to phosphine. A coordinatively-unsaturated species can be formed endothermically from $RuCl(OCH_3)(MeOH)(PH_3)_3$ by methanol dissociation; the stereoisomer of $RuCl(OCH_3)(PH_3)_3$ with a vacant site trans-disposed to the Cl ligand was stabilized by the presence of an agostic interaction between CH^β and Ru. Dissociation of the methoxy C–H bond in $RuCl(OCH_3)(PH_3)_3$ was exothermic according to the MP2 method, irrespective of coordination modes of the methoxy ligand. These ab initio calculations on the stereochemical reaction paths are very consistent with the conclusion deduced from the observed methanol dehydrogenation with the $Ru(OAc)Cl(PEtPh_2)_3$ catalyst.

Introduction

Homogeneous catalysts for alcohol dehydrogenation have been explored extensively under both thermal[1] and photochemical[2] conditions. However, active and selective catalysts for methanol dehydrogenation were scarcely reported because of its high endothermicity and the product reactivity. Under photoirradiation, carbon monoxide,[3a] ethylene glycol,[3b-d] and dimethoxymethane[3c,d,h] and formaldehyde[3c,d] were yielded with some catalysts. Under boiling conditions, methyl formate and dimethoxymethane were obtained thermally with $RuCl_2(PPh_3)_3$.[3f]

With $Ru(OAc)Cl(PEtPh_2)_3$, the catalyst of the present study, formaldehyde is formed selectively at an initial turnover frequency of 0.29 h^{-1};[3e]

$$CH_3OH \rightarrow HCHO + H_2 \quad (1)$$

The following catalytic cycle has been proposed for this reaction:[3g] (1) the OAc ligand is substituted with a methoxy ligand from methanol, releasing free acetic acid, (2) a cis-disposed vacant site thus generated is utilized for C–H bond dissociation of the OCH_3 ligand, and (3) the HOAc attack to the hydride intermediate regenerates the original complex, liberating dihydrogen.

A gradual decrease in catalytic activity is caused by conversion of $Ru(OAc)Cl(PEtPh_2)_3$ to $RuCl(H)(CO)(PEtPh_2)_3$, for which the trans-disposed structure between the CO and Cl ligands has been verified by an NMR analysis.[3g] Formation of the latter complex is accelerated by addition of paraformaldehyde to the catalyst solution, with accompanying deactivation.

As shown in Scheme I, if one follows the above-proposed mechanism, one has to assume two possible stereochemical reaction paths; a vacant site used for coordination of methanol, methoxy, or formaldehyde is trans-disposed either to the phosphine ligand (path P) or to the chloride ligand (path Cl). Formaldehyde, once η^2-coordinated to the vacant site, is known to be converted into a CO ligand, forming a Ru–C bond.[4] The observed trans stereochemistry of $RuCl(H)(CO)(PEtPh_2)_3$ requires that this species is formed along path Cl during the catalyst deactivation, whereas the catalytic cycle must proceed along path P.[5]

Organotransition metal catalysts have been studied extensively in the last decade with ab initio molecular

† University of Tokyo.
‡ IMS.

(1) (a) Charman, H. B. *J. Chem. Soc. B* **1970**, 584. (b) Strohmeier, W.; Hitzel, E.; Kraft, B. *J. Mol. Catal.* **1977**, *3*, 61. (c) Dobson, A.; Robinson, S. D. *Inorg. Chem.* **1977**, *16*, 137. (d) Fragale, C.; Gargano, M.; Rossi, M. *J. Mol. Catal.* **1979**, *5*, 65. (e) Jung, C. W.; Garrou, P. E. *Organometallics* **1982**, *1*, 658. (f) Shinoda, S.; Kojima, T.; Saito, Y. *J. Mol. Catal.* **1983**, *99*, 18.

(2) (a) Shinoda, S.; Moriyama, H.; Kise, Y.; Saito, Y. *J. Chem. Soc., Chem. Commun.* **1978**, 384. (b) Arakawa, H.; Sugi, Y. *Chem. Lett.* **1981**, 1323. (c) Moriyama, H.; Aoki, T.; Shinoda, S.; Saito, Y. *J. Chem. Soc., Perkin Trans 2* **1982**, 369. (d) Irie, R.; Li, X.; Saito, Y. *J. Mol. Catal.* **1983**, *18*, 263. (e) Griggs, C. G.; Smith, D. J. H. *J. Organomet. Chem.* **1984**, *273*, 105. (f) Roundhill, D. M. *J. Am. Chem. Soc.* **1985**, *107*, 4354. (g) Yamakawa, T.; Miyake, H.; Moriyama, H.; Shinoda, S.; Saito, Y. *J. Chem. Soc., Chem. Commun.* **1986**, 326. (h) Yamakawa, T.; Katsurao, T.; Shinoda, S.; Saito, Y. *J. Mol. Catal.* **1987**, *42*, 183. (i) Nokuma, K.; Saito, Y. *J. Mol. Catal.* **1989**, *52*, 99.

(3) (a) Delgalo-Lieta, E.; Luke, M. A.; Jones, R. F.; Cole-Hamilton, D. J. *Polyhedron* **1982**, *1*, 839. (b) Arakawa, H.; Sugi, Y.; Takeuch, K.; Bando, K.; Takami, Y. *Shokubai* **1983**, *25*, 392. (c) Yamamoto, H.; Shinoda, S.; Saito, Y. *J. Mol. Catal.* **1985**, *30*, 259. (d) Takahashi, T.; Shinoda, S.; Saito, Y. *J. Mol. Catal.* **1985**, *31*, 301. (e) Shinoda, S.; Itagaki, H.; Saito, Y. *J. Chem. Soc., Chem. Commun.* **1985**, 860. (f) Smith, T. A.; Aplin, R. P.; Maitlis, P. M. *J. Organomet. Chem.* **1985**, *291*, C13. (g) Itagaki, H.; Shinoda, S.; Saito, Y. *Bull. Chem. Soc. Jpn.* **1988**, *61*, 2991. (h) Nomura, K.; Saito, Y.; Shinoda, S. *J. Mol. Catal.* **1989**, *50*, 303.

(4) Chaudret, B. N.; Cole-Hamilton, D. J.; Nohr, R. S.; Wilkinson, G. *J. Chem. Soc., Dalton Trans.* **1977**, 1546.

(5) Itagaki, H.; Saito, Y.; Shinoda, S. *J. Mol. Catal.* **1987**, *41*, 209.

0276-7333/93/2312-1648$04.00/0

Scheme I. Possible Reaction Paths for Methanol Dehydrogenation with Ru(OAc)Cl(PEtPh$_2$)$_3$

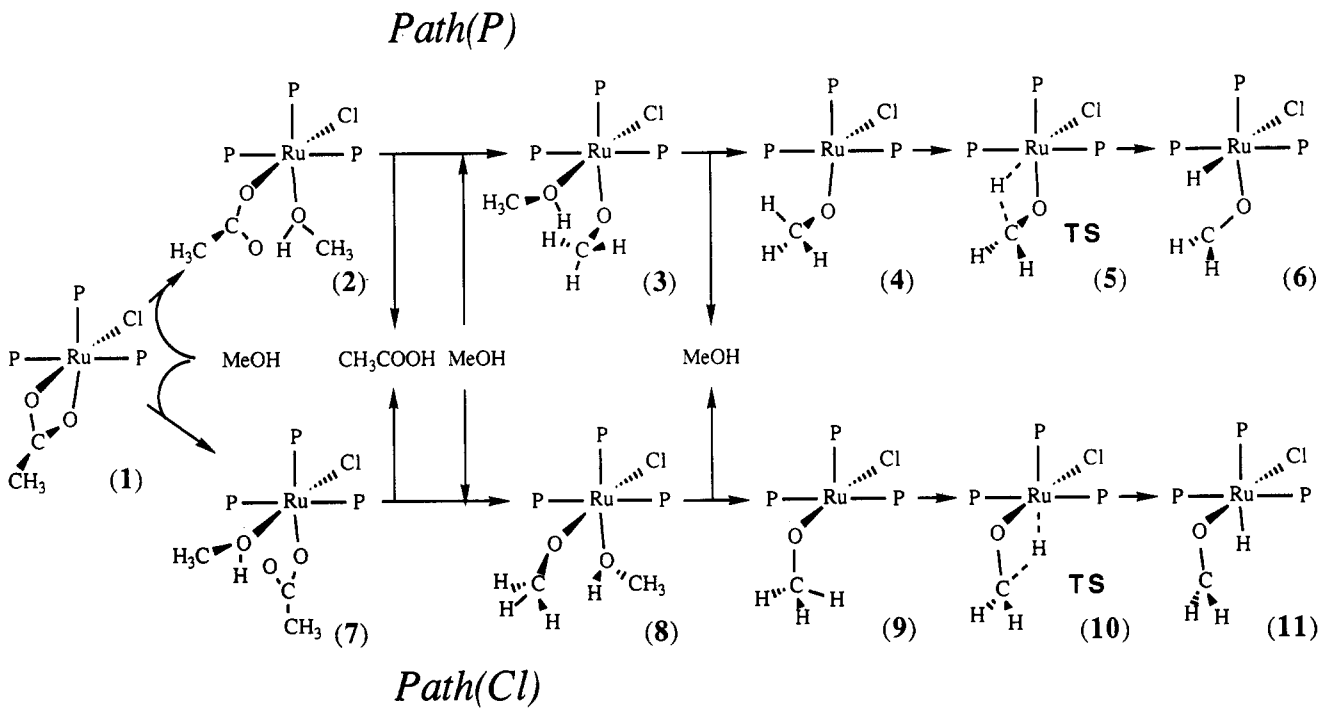

orbital methods,[6] where it has been shown that theoretical calculations can elucidate the mechanism of catalytic as well as elementary organometallic reactions successfully. In this paper, with ab initio MO calculations we compare the above mentioned two reaction paths, in order to clarify theoretically which path is actually more favorable. The energy difference between the two paths may be interpreted in terms of the trans influence of each ligand. Accordingly, we pay attention to the difference in trans influence among ligands.

Methods of Calculation

Two basis sets, represented as I and II, were used. The smaller basis set I was constructed from split valence basis functions [2s2p2d]/(3s3p4d)[7] for Ru, 3-21G[8] sets for the OAc, OCH_3, and MeOH ligands, and STO-2G[9] for spectator ligands PH_3 and Cl. The larger basis set II was constructed as follows. Basis functions [2s2p3d]/(3s3p4d),[7] a triple-ζ contraction for the d orbitals, were adopted for the valence electrons of Ru. As for OAc, OCH_3, and MeOH ligands, split valence basis functions [3s2p]/(8s5p)[10] for O and C atoms and triple-ζ basis functions [3s]/(4s)[11] for H were used, to which a single d and p polarization functions, respectively, were added.[10] The split valence basis functions [4s3p]/(11s8p)[10] for spectator ligands P and Cl and the double-ζ basis functions [2s]/(4s)[11] for the H atom of the PH_3 ligand were employed. In both basis sets, the relativistic effective core potential determined by Hay and Wadt[7] was used for the core (up to 4p) electrons of the Ru atom. For simplicity, we used the notation in which RHF/I, for instance, represents RHF calculation using the basis set I.

Full geometry optimization was carried out at the RHF/I level under C_s symmetry using the GAUSSIAN82[12] program with the energy gradient method.[13] In order to calculate the energy profile more reliably, further calculations were carried out for the processes of methanol dissociation and C–H bond splitting at the second-order Möller–Plesset (MP2)/II level with the geometries optimized at the RHF/I level.

Localized molecular orbitals (LMO's) were also calculated for the valence orbitals by the Boys procedure,[14] so as to examine the sequential change of the chemical bonding nature during the CH bond splitting of the methoxy ligand.

Results and Discussion

All the species involved in Scheme I are d^6 electron systems, which have the orbital diagrams shown in Scheme

(6) (a) Koga, N.; Morokuma, K. *Topics Phys. Organomet. Chem.* **1989**, *3*, 1 and references therein. (b) Hay, P. J. *J. Am. Chem. Soc.* **1987**, *109*, 705. (c) Antolovic, D.; Davidson, E. R. *J. Am. Chem. Soc.* **1987**, *109*, 5828. (d) Sakaki, S.; Dedieu, A. *Inorg. Chem.* **1987**, *26*, 3278. (e) Rosi, M.; Sgamellotti, A.; Tarantelli, F.; Floriani, C.; Guest, M. F. *J. Chem. Soc., Dalton Trans.* **1988**, 321. (f) Nakamura, S.; Morokuma, K.; *Organometallics* **1988**, *7*, 1904. (g) Sakaki, S.; Ohkubo, K. *Inorg. Chem.* **1988**, *27*, 2020. (h) Koga, N.; Jin, S. Q.; Morokuma, K. *J. Am. Chem. Soc.* **1988**, *110*, 3417. (i) Daniel, C.; Koga, N.; Han, J.; Fu, X. Y.; Morokuma, K. *J. Am. Chem. Soc.* **1988**, *110*, 3773. (j) Sakaki, S.; Aizawa, T.; Koga, N.; Morokuma, K.; Ohkubo, K. *Inorg. Chem.* **1989**, *28*, 103. (k) Sakaki, S.; Ohkubo, K. *J. Phys. Chem.* **1989**, *93*, 5655. (l) Pacchioni, G. *J. Am. Chem. Soc.* **1990**, *112*, 80. (m) Versluis, L.; Ziegler, T. *Organometallics* **1990**, *9*, 2985. (n) Sakaki, S.; Koga, N.; Morokuma, K. *Inorg. Chem.* **1990**, *29*, 3110. (o) Sakaki, S. *J. Am. Chem. Soc.* **1990**, *112*, 7813. (p) Koga, N.; Morokuma, K. *J. Phys. Chem.* **1990**, *94*, 5454. (q) Koga, N.; Morokuma, K. *Chem. Rev.* **1991**, *91*, 823. (r) Koga, N.; Morokuma, K. *Organometallics* **1991**, *10*, 946. (s) Morokuma, K.; Borden, W. T. *J. Am. Chem. Soc.* **1991**, *113*, 1912. (t) Maseras, F.; Duran, M.; Lledós, A.; Bertrán, J. *J. Am. Chem. Soc.* **1991**, *113*, 2879. (u) Sakaki, S.; Ieki, M. *Inorg. Chem.* **1991**, *30*, 4218. (v) Haynes, G. R.; Martin, R. L.; Hay, P. J. *J. Am. Chem. Soc.* **1992**, *114*, 28. (w) Sakaki, S. *J. Am. Chem. Soc.* **1992**, *114*, 2055. (x) Kawamura-Kuribayashi, H.; Koga, N.; Morokuma, K. *J. Am. Chem. Soc.* **1992**, *114*, 2359. (y) Lin, Z.; Hall, M. B. *J. Am. Chem. Soc.* **1992**, *114*, 2928.

(7) Hay, P. J.; Wadt, W. R. *J. Chem. Phys.* **1985**, *82*, 270.

(8) Binkley, J. S.; Pople, J. A.; Hehre, W. J. *J. Am. Chem. Soc.* **1980**, *102*, 939.

(9) Hehre, W. J.; Stewart, R. F.; Pople, J. A. *J. Chem. Phys.* **1969**, *51*, 2657. The use of a small basis set for ligands not directly involved in the reaction has been justified in references such as 4h and 4i.

(10) Huzinaga, S.; Andzelm, J.; Klobukowski, M.; Radzio-Andzelm, E.; Sakai, Y.; Tatewaki, H. *Gaussian Basis Sets for Molecular Calculations*; Elsevier: Amsterdam, 1984.

(11) Dunning, T. H. *J. Chem. Phys.* **1970**, *53*, 2823.

(12) Binkley, J. S.; Frisch, M. J.; DeFrees, D. J.; Raghavachari, K.; Whiteside, R. A.; Schlegel, H. B.; Pople, J. A. *GAUSSIAN82*; Carnegie-Mellon Chemistry Publishing Unit: Pittsburgh, PA, 1984.

(13) Kitaura, K.; Obara, S.; Morokuma, K. *Chem. Phys. Lett.* **1981**, *77*, 452.

(14) Boys, S. F. In *Quantum Theory of Atoms, Molecules and the Solid State*; Lowdin, P. O., Ed.; Academic Press: New York, 1968.

Scheme II

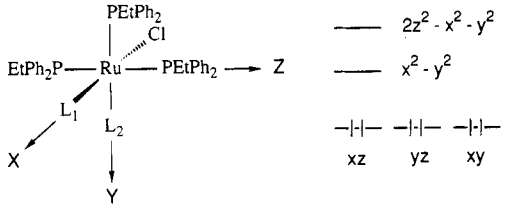

Scheme III

II. Three π orbitals, xz, yz, and xy, are occupied, and two σ orbitals, $x^2 - y^2$ and $2z^2 - x^2 - y^2$, are vacant, with their relative energies depending on the ligands L_1 and L_2. As will be discussed later, we have found the orders of trans influence to be H > CH_3O > η^1-OAc > H_2CO, CH_3OH > η^2-OAc, and PH_3 > Cl.

Since the stereochemistry of phosphine coordination of related complexes, $RuCl(H)(CO)(PEtPh_2)_3$ (cf. Scheme III and vide infra) and $Ru(\eta^2\text{-OAc})(H)(PPh_3)_3$,[15] was meridional, three phosphine ligands are set at the meridional positions in the present calculation. We use PH_3 in place of the actual ligand $PEtPh_2$ for computational limitation.

1. Structure of the Starting Catalyst Species: Ru(η^2-OAc)Cl(PH_3)$_3$. The structure of the starting catalytic species (1) optimized at the RHF/I level is shown in Figure 1. It is in reasonable agreement with the X-ray structure of the related complex, $Ru(OAc)(H)(PPh_3)_3$.[15] The Ru–O bond distances (trans to P, 2.19 Å; trans to Cl, 2.16 Å) in 1 agree with those observed (trans to P, 2.21 Å; trans to H, 2.20 Å) in $Ru(OAc)(H)(PPh_3)_3$. These Ru–O bonds in 1 are relatively long, in comparison with those in other complexes in Scheme I, as will be discussed later, indicating that coordination of the acetato ligand is not strong. Moreover, the stronger trans influence of P relative to Cl is reflected in the larger Ru–O distance which is trans to P relative to that trans to Cl. A poorer agreement is seen, as expected, for the Ru–P bond distances where a minimal basis set is used for PH_3. Agreement in bond angles (O–Ru–O 60.1° vs 57.6° or O–C–O 118.1° vs 115°) is also quite good.

2. Methanol Coordination to the Catalyst: Ru(η^2-OAc)Cl(PH_3)$_3$ + MeOH → Ru(η^1-OAc)Cl(MeOH)(PH_3)$_3$. Methanol coordination to $Ru(\eta^2\text{-OAc})Cl(PEtPh_2)_3$ would be accomplished by generating a vacant site, the acetato ligand being changed from dihapto to monohapto. Two stereochemical isomers (2 and 7) are, therefore, possible for the presumed intermediate, $Ru(\eta^1\text{-OAc})Cl(MeOH)(PEtPh_2)_3$; their optimized geometries are shown in Figure 2. In these complexes, the monodentate acetato group can rotate around the C–O bond interacting with Ru and also methanol can rotate around the Ru–O bond. The structures shown in Figure 2, with hydrogen bonding between an acetato oxygen atom and the methanol OH bond, were assumed, since they are expected to be the most stable due to the hydrogen bonding. The O—C—O

(15) Skapski, A. C.; Stephens, F. A. *J. Chem. Soc., Dalton Trans.* **1974**, 390.

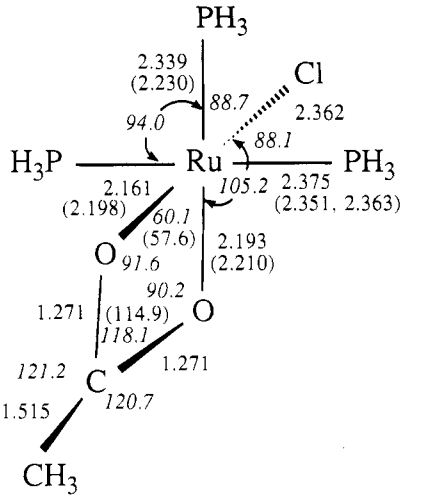

(1)

Figure 1. Optimized geometry of $Ru(\eta^2\text{-OAc})Cl(PH_3)_3$ (1). The bond distances are in angstroms, and angles, in degrees. Experimental values of $Ru(OAc)(H)(PPh_3)_3$ are in parentheses.

bond angle opens up from 118.1° for the bidentate OAc ligand in 1 to 125.5° in 2 and 124.8° in 7 for the monodentate ligand, and the Ru—O bond distance shortens from 2.16 and 2.19 Å in 1 to 2.11 Å in both 2 and 7. Molecular distortion due to bidentate-ligand coordination, if any, would be relaxed by these structural changes. In 2 the difference in distance between two CO bonds in the OAc ligand is 0.014 Å, whereas that in 7 is only 0.001 Å; the OAc ligand in 7 is still similar to the OAc anion as in 1, whereas that in 2 has a character of nonequivalent C=O and C—O bonds. In 7 the stronger trans influence of the PH_3 ligand results in a larger OAc anion character. On the other hand, in 2 the weaker trans influence of Cl makes the Ru—O bond more covalent.

Two "$RuCl(PH_3)_3$" fragments in 2 and 7 display little difference. The Ru–Cl, Ru–P(trans to O), and Ru–P(trans to P) distances are the same within 0.004 Å between 2 and 7, and the P–Ru–P and Cl–Ru–P(trans to P) bond angles are same within 1°. The only exception is the Cl–Ru–P(trans to O) bond angles, where the differences is about 5°. One also notices that the Ru–OAc distance is the same between 2 and 7, regardless of the difference in the trans ligand. However, the Ru–$OHCH_3$ distance seems to depend substantially on the trans ligand; the distance trans to Cl in 7 is 0.021 Å longer than that trans to PH_3 in 2. They are not consistent with the general trend that the trans influence of Cl is weaker than that of PH_3. This may be ascribed to hydrogen bonding between the OAc and the MeOH ligand. The short OH···O distances of 1.515 and 1.447 Å and the O···O distances of 2.480 and 2.451 Å in 2 and 7, respectively, show that interaction between OH and O is very strong. The long OH distances of 1.012 and 1.031 Å in 2 and 7, respectively, also support this. The Ru–OAc and Ru–OHMe distances might have been adjusted to make hydrogen bond stabilization maximum.

As shown in Table I, the exothermic coordination energies of methanol to 1 are 33.3 and 27.5 kcal/mol in path P and path Cl, respectively, at the RHF/I level. The coordination structure 2 is energetically more stable than 7 by 5.8 kcal/mol. As shown later, the η^1-OAc ligand has a stronger trans influence than CH_3OH. Energetically more favorable is the case where the ligand with stronger

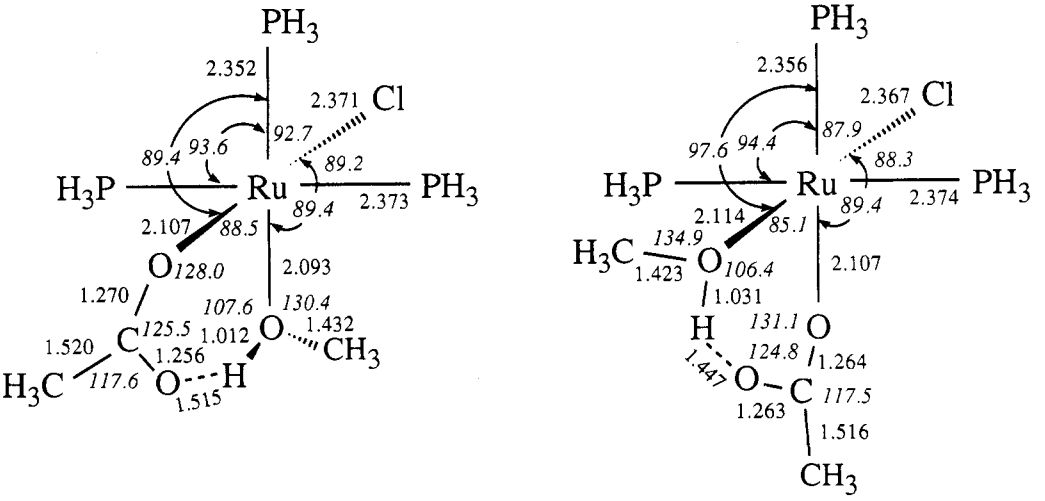

(2) (7)

Figure 2. Optimized geometries (in Å and deg) of Ru(η^1-OAc)Cl(MeOH)(PH$_3$)$_3$ (**2** and **7**).

Table I. Relative Energies (kcal/mol) for Methanol Coordination to Ru(η^2-OAc)Cl(PH$_3$)$_3$[a]

Ru(η^2-OAc)Cl(PH$_3$)$_3$ (**1**)[b] + MeOH[c]	Ru(η^1-OAc)Cl(MeOH)(PH$_3$)$_3$	
	2	**7**
0.0	−33.3	−27.5

[a] Calculated at the RHF/I level. [b] Ru(η^2-OAc)Cl(PH$_3$)$_3$ (**1**): −1672.8343 hartrees. [c] MeOH: −114.3980 hartrees.

trans influence and that with weaker trans influence are located trans to each other; **2** with trans η^1-OAc and Cl is the case.

The energetic difference between the methanol-coordinated intermediates, **2** and **7**, allows us to propose a predominant attack of methanol at the site trans-disposed to PEtPh$_2$ of Ru(OAc)Cl(PEtPh$_2$)$_3$ at the beginning of the catalysis cycle.

The strong hydrogen bonding discussed above suggests the succeeding step of acetic acid dissociation is an easy process (cf. Scheme I). Also, in such a step the effect of solvent would be essential. In addition, the next step of MeOH coordination may couple with acetic acid dissociation. The situation would be complicated. Therefore, we have not studied these two steps any further.

3. Structure of Reaction Intermediate RuCl(OCH$_3$)(MeOH)(PH$_3$)$_3$. As soon as the acetato ligand dissociates from Ru(η^1-OAc)Cl(MeOH)(PEtPh$_2$)$_3$ as free acetic acid, the vacant site of the coordinatively-unsaturated intermediate, RuCl(OCH$_3$)(PEtPh$_2$)$_3$, is presumably coordinated with a solvent methanol molecule (cf. Scheme I). Two stereochemical isomers of RuCl(OCH$_3$)(MeOH)(PH$_3$)$_3$ are now investigated.

As shown in Figure 3, the methoxy O–Ru distance, 2.05 Å, in **3** and **8** is substantially shorter than the acetato O–Ru distance, 2.11 Å, in **2** and **7** and the methanol O–Ru distance, 2.09–2.15 Å, in **2**, **3**, **7**, and **8**, indicating that the methoxy O–Ru bond is stronger than the other O–Ru bonds. The stronger bond is expected to have a stronger trans influence, and this is actually what is observed. The Ru–Cl distance trans-disposed to methoxy in **8** is about 0.02 Å longer than Ru–Cl distances trans to methanol or acetyl in **2**, **3**, and **7**, and the Ru–P distance trans to methoxy in **3** is 0.01–0.03 Å longer than the Ru–P distance trans to methanol or acetyl.

In **8**, the methoxy ligand with strong trans influence is located trans to Cl, with weak trans influence. Therefore, **8** is more stable than **3** by 5.2 kcal/mol at the MP2/II level, as shown in Table II.

4. C–H Bond Splitting in RuCl(OCH$_3$)(PH$_3$)$_3$. A vacant site necessary for C–H bond splitting is generated if the methanol ligand is dissociated from the RuCl(OCH$_3$)(MeOH)(PH$_3$)$_3$ intermediate complex, leaving the methoxy ligand next to the vacant site (cf. Scheme I). Actually, the methanol dissociation may take place concurrently with the methoxy C–H activation. It is, however, convenient to examine the dissociation step separately as a limiting case. The geometries of the reactant methoxy complex RuCl(OCH$_3$)(PH$_3$)$_3$, the C–H activation product HRuCl(CH$_2$O)(PH$_3$)$_3$, and the transition state connecting them have been optimized for path P and path Cl as shown in Figures 4 and 5, respectively. The energetics of CH bond splitting as well as methanol dissociation will be discussed later.

There are remarkable differences between the two structures, **4** and **9**, of the coordinately unsaturated methoxy complex. Long C–H$^\beta$ (1.14 Å) and short H$^\beta$–Ru (2.16 Å) distances and a small Ru–O–C bond angle (92.4°) in **4** are evidences for a CH$^\beta$···Ru agostic interaction.[16,17] In contrast, no agostic interaction is found for **9** with normal C–H (1.10 Å) and long Ru–H (2.84 Å) distances as well as the normal angle Ru–O–C (115.4°). This difference can be understood as the difference in trans influence. The vacant d orbital to be involved in the agostic interaction is the $x^2 - y^2$ orbital (cf. Scheme II and vide infra). In **4** the ligand trans to the agostic CH bond is Cl, with weak trans influence. Therefore, in **4** the stronger electron donation can take place. In addition, in **9** the strong CH$_3$O–Ru bond due to the weak trans influence of Cl makes the structural distortion even more difficult.

(16) (a) Cotton, F. A.; LaCour, T.; Stanislowski, A. G. *J. Am. Chem. Soc.* **1974**, *96*, 754. (b) Dawoodi, Z.; Green, M. L. H.; Mtetwa, V. S. B.; Prout, K. *J. Chem. Soc., Chem. Commun.* **1982**, 802. (c) Brookhart, M.; Green, M. L. H. *J. Organomet. Chem.* **1983**, *250*, 395.

(17) (a) Koga, N.; Obara, S.; Morokuma, K. *J. Am. Chem. Soc.* **1984**, *106*, 4625. (b) Obara, S.; Koga, N.; Morokuma, K. *J. Organomet. Chem.* **1984**, *270*, C33. (c) Koga, N.; Obara, S.; Kitaura, K.; Morokuma, K. *J. Am. Chem. Soc.* **1985**, *107*, 7109. (d) Koga, N.; Morokuma, K. *J. Am. Chem. Soc.* **1988**, *110*, 108.

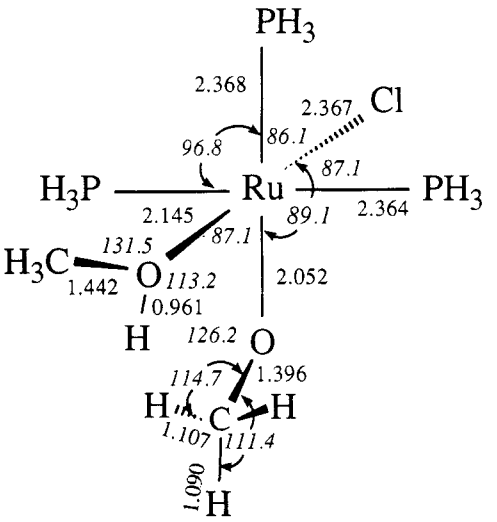

(3)

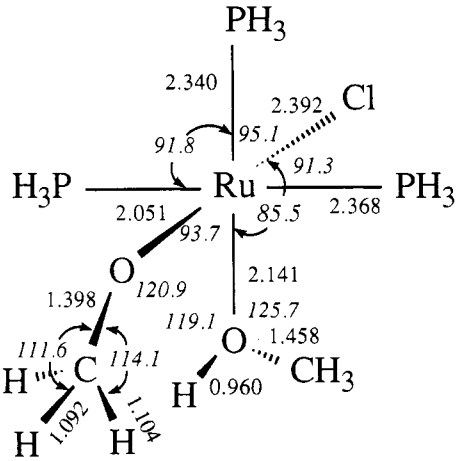

(8)

Figure 3. Optimized geometries (in Å and deg) of $RuCl(OCH_3)(MeOH)(PH_3)_3$ (**3** and **8**).

Table II. Relative Energies (kcal/mol) from the Methanol Dissociation to the C–H Bond Splitting Process

complex	RHF/I[a]	RHF/II[a]	MP2/II[a]
$RuCl(OCH_3)(MeOH)(PH_3)_3$ (**3**)	11.8	7.1	5.2
(**8**)[b]	0.0	0.0	0.0
$RuCl(OCH_3)(PH_3)_3$ (**4**) + MeOH[c]	38.9	21.0	22.0
(**9**) + MeOH	31.0	17.0	27.6
$RuCl(OCH_2\cdots H)(PH_3)_3$ (**5**) + MeOH	52.0	29.8	12.2
(**10**) + MeOH	53.4	29.9	16.8
$HRu(CH_2O)(PH_3)_3$ (**6**) + MeOH	50.7	31.6	4.0
(**11**) + MeOH	50.1	30.6	2.1

[a] Energies were calculated with the RHF method using basis set I (RHF/I) and basis set II (RHF/II) and with the MP2 method using basis set II (MP2/II). [b] $RuCl(OCH_3)(MeOH)(PH_3)_3$ (**8**): −1675.0903 (RHF/I), −1732.2213 (RHF/II), and −1733.2743 (MP2/II) hartrees. [c] MeOH: −114.3980 (RHF/I), −115.0419 (RHF/II), and −115.3822 (MP2/II) hartrees.

Now we examine structures of the product, formaldehyde complexes, **6** and **11**. In both complexes the Ru–C distance (2.15 Å (**6**) and 2.13 Å (**11**)) is not very different from the Ru–O distance (2.09 Å (**6**) and 2.08 Å (**11**)), indicating η^2-type H_2CO coordination. The Ru–H_2CO distance in **11** is shorter than that in **6**, consistent with the weaker trans influence of Cl which is trans to H_2CO in **11**. On the other hand, in **6** the Ru–H_2CO bond is weak and thus formaldehyde retains an ability to bond to others. As a result, the Ru–H bond interacts with the carbon of formaldehyde, as will be shown in the next section. This interaction lengthens the Ru–H bond, which is longer than that in **11**, although the trans ligand is Cl, with weak trans influence. The Ru–H, C–H, and C–O distances of the transition states, **5** and **10**, more closely resemble the products, **6** and **11**, than the reactants, **4** and **9**, suggesting that the transition state is relatively late.

5. Localized Molecular Orbital Analysis of the C–H Bond Splitting Mechanism. In order to analyze the C–H bond splitting mechanism, Boys localized molecular orbitals (LMO's) were calculated for **4**–**6** of reaction path P. The occupied LMO's participating in bond exchange are shown in Figure 6.

An electron-donative interaction from the CH bond to the vacant d orbital of the Ru atom, the origin of the $CH^{\beta}\cdots Ru$ agostic interaction, takes place in the reactant (Figure 6a). Parts b and c of Figure 6 show a lone pair occupied d_{xy} orbital, which does not interact with the CH_3O ligand, and the Ru–O σ bond, respectively.

At the transition state, the CH bond is stretched substantially, and hence electron donation from the CH σ orbital to the vacant $d_{x^2-y^2}$ orbital takes place (Figure 6d) much more than at the reactant (Figure 6a), resulting in substantial formation of a dσ-type RuH bond. Also, the σ^* orbital of the stretched CH bond as well as the π^* orbital of the partially formed CO π bond accept electrons from the lone pair d_{xy} orbital (Figure 6e). This back-donation in cooperation with the donation above reorganizes electron pairing and causes the CH bond splitting. In addition, the π orbital of the partially formed CO π bond donates the electrons into the vacant $d_{x^2-y^2}$ orbital (Figure 6f). At the transition state, donation and back-donation have already taken place substantially, consistent with its lateness. In the product the Ru–H σ bond is formed (Figure 6g), and donation and back-donation are responsible for the Ru–H_2CO bond (Figure 6h,i). Figure 6g shows an interesting interaction of the Ru–H bond with the carbon of formaldehyde, as discussed in the preceding section.

6. Potential Energy Profile for Methanol Dissociation and C–H Bond Splitting: $Ru(OCH_3)Cl(MeOH)(PH_3)_3$ → $Ru(OCH_3)Cl(PH_3)_3$ + MeOH → $RuCl(H)(HCHO)(PH_3)_3$ + MeOH. Energies of methanol dissociation and CH bond splitting, essential steps in the present catalytic reaction, are discussed in this section, and the activation barriers and energies of reaction are compared between two reaction paths. The energies relative to **8** calculated at the several levels are shown in Table II, and the potential energy profile at the MP2/II level, which is more reliable than that at the RHF level, is depicted in Figure 7.

Methanol dissociation from $RuCl(OCH_3)(MeOH)(PH_3)_3$, generating $RuCl(OCH_3)(PH_3)_3$, is endothermic: 16.8 and 27.6 kcal/mol in path P (**3** → **4**) and path Cl (**8** → **9**), respectively, at the MP2 level. The instability of coordinatively-unsaturated species is reasonably confirmed. Comparison between the MP2/II and the RHF/II endothermicity shows that the electron correlation strengthens the Ru–methanol bond. Methanol dissociation in path P is easier than in path Cl, although in path

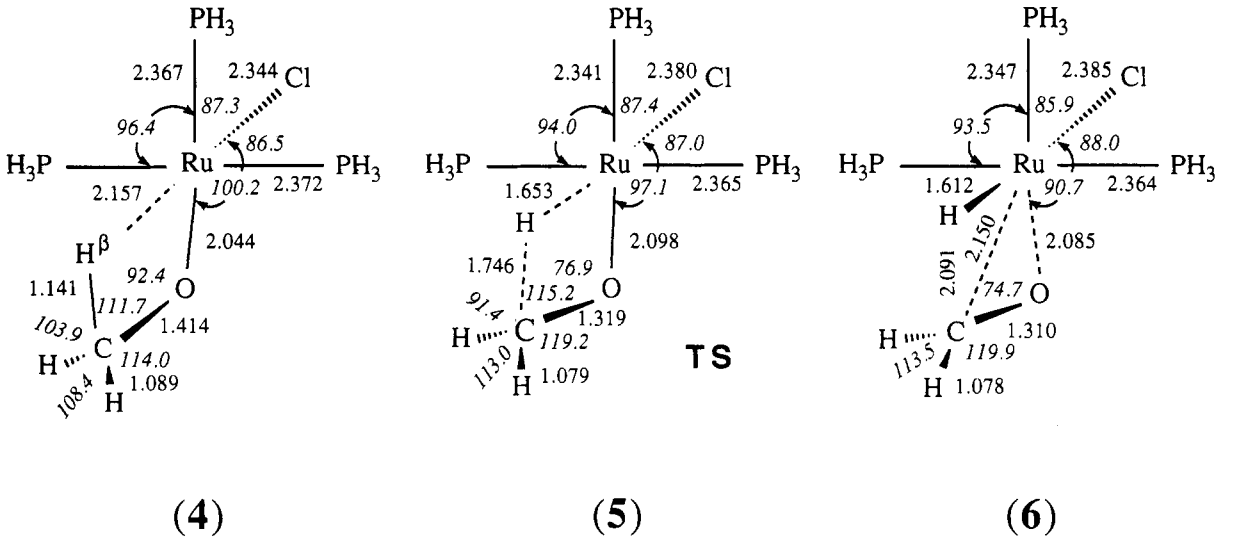

Figure 4. Optimized geometries (in Å and deg) of RuCl(OCH$_3$)(PH$_3$)$_3$ (**4**), transition state **5**, and HRuCl(CH$_2$O)(PH$_3$)$_3$ (**6**) for path P.

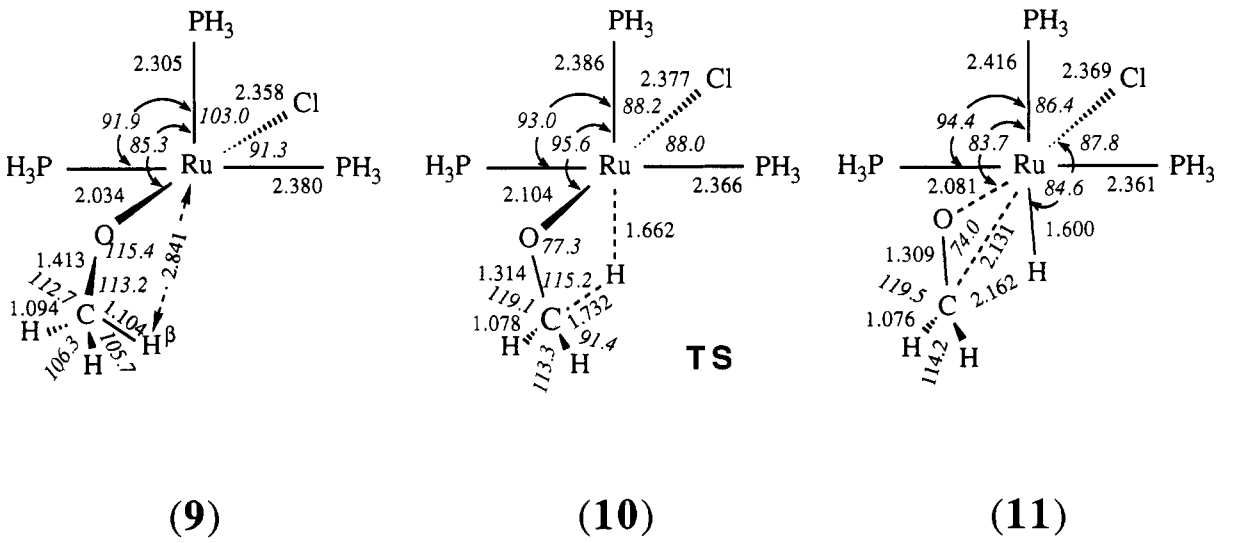

Figure 5. Optimized geometries (in Å and deg) of RuCl(OCH$_3$)(PH$_3$)$_3$ (**9**), transition state **10**, and HRuCl(CH$_2$O)(PH$_3$)$_3$ (**11**) for path Cl.

P the ligand trans to dissociating methanol is Cl, with weak trans influence. This is ascribed to the facts that **4** is more stable than **9** by 5.6 kcal/mol (MP2/II) and that **3** is less stable than **8** by 5.2 kcal/mol (MP2/II). The stability of **4** is caused by the CH$^\beta$···Ru agostic interaction.

At the RHF level, agostic **4** is less stable than nonagostic **9** by 7.9 and 4.0 kcal/mol at the RHF/I and RHF/II levels, respectively. The electron correlation effects enhance electron-donative interaction, as expected, resulting in agostic **4** being more stable than nonagostic **9**. A possibility of CH$^\beta$···Ru agostic interaction in the intermediate **9** was inspected virtually by assuming an agostic structure, where only the Ru–O–C angle and the CH$^\beta$ distance in **9** were replaced by corresponding values in the intermediate **4**. This structural change induced 0.7 kcal/mol stabilization at the MP2/II level. This suggests that at the more reliable MP2 level a weak agostic interaction would take place in **9**.

The C–H bond splitting process (**4** → **6** in path P, **9** → **11** in path Cl) calculated with the MP2/II method was exothermic without any energy barrier (Figure 7); the RHF/I transition states, **5** and **10**, are lower in MP2/II energy than the reactants, **4** and **9**, respectively, and are not really transition states. However, the energy barrier for the combined step (**3** → **6** in path P and **8** → **11** in path Cl) of methanol dissociation and C–H bond splitting is positive and is smaller in path P than in path Cl: 16.8 kcal/mol in path P (**3** → **4** + MeOH) and 27.6 kcal/mol in path Cl (**8** → **9** + MeOH) with the MP2/II method. The MP2/II barrier comes from methanol dissociation. The electron correlation effect, which enhances donation and back-donation in the Ru–H$_2$CO bond, stabilizes **6** and **11** very much, to make the CH bond splitting downhill. Therefore, the lower barrier in path P is ascribed in part to the stronger trans influence of PH$_3$, which destabilizes **3**, and in part to the weaker trans influence of Cl, which stabilizes **4**, as discussed above.

7. Trans Influence. We summarize in Table III the Ru–O, Ru–C, and Ru–H bond distances in various intermediates, in order to compare the trans influence of PH$_3$ and Cl. As discussed previously, in **2** and **7** strong hydrogen bonding takes place, which affects the Ru–O bond distances. In **6** the Ru–H bond interacts with the carbon of H$_2$CO, resulting in the long distance. Neglecting these exceptions, generally, the Ru–ligand bond trans to the Ru–PH$_3$ bond is longer than that trans to the Ru–Cl

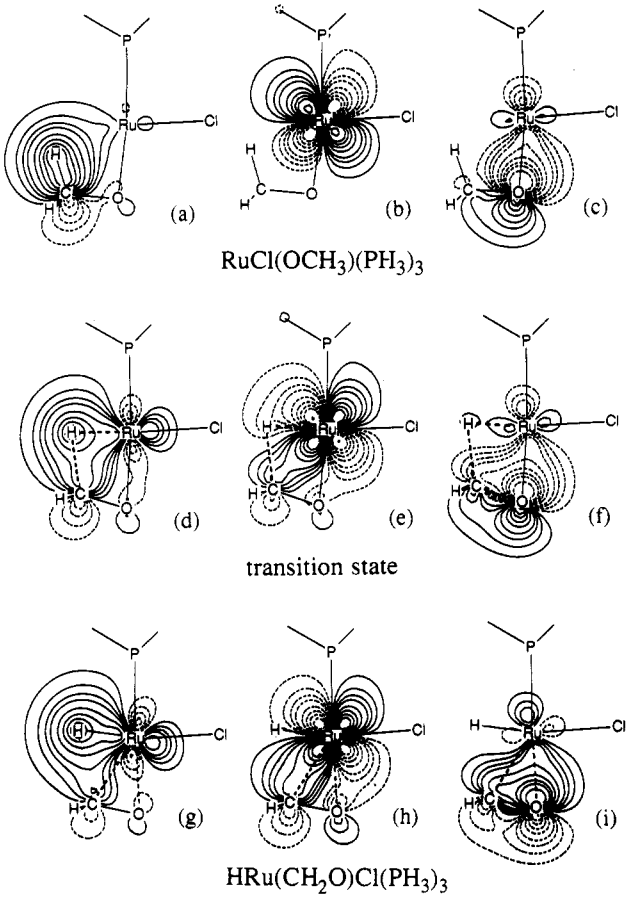

Figure 6. LMO's representing the bonding nature of the OCH_3 ligand during the CH bond splitting process in $RuCl(OCH_3)(PH_3)_3$ along path P.

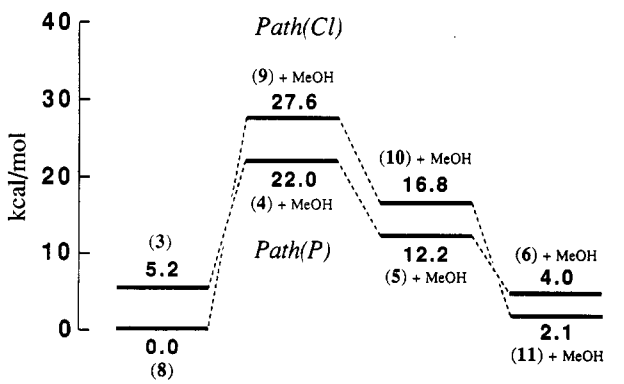

Figure 7. Energy profiles from the methanol dissociation to the CH bond splitting process.

bond; PH_3 has a stronger trans influence than Cl. Also, in Table IV we compare the Ru–Cl and Ru–P bond distances as functions of various trans ligands. Neglecting the case of H in **6** and CH_3OH in **2** and **7**, we can reduce the order of trans influence: H > CH_3O > η^1-OAc > H_2CO and CH_3OH > η^2-OAc.

8. Concluding Remarks on Consistency between Experimental and Calculated Results in Catalysis. Gradual deactivation owing to the change from $Ru(OAc)Cl(PEtPh_2)_3$ to $RuCl(H)(CO)(PEtPh_2)_3$ was accelerated by the addition of paraformaldehyde to the catalyst solution.[3g] According to NMR analysis, the CO and Cl ligands were mutually trans-disposed (Scheme III). After η^2-type coordination to the vacant site, formaldehyde would decompose finally to a CO ligand via CHO, keeping the position of coordination.[4] Consequently, the observed

Table III. Distances (Å) of the Ru–O, Ru–C, and Ru–H Bonds Trans to the Ru–P and Ru–Cl Bonds in Various Intermediates

		bond distance	
bond	ligand	PH_3	Cl
Ru–O	η^2-OAc	2.193 (**1**)	2.161 (**1**)
	η^1-OAc	2.107 (**7**)	2.107 (**2**)
	CH_3OH	2.093 (**2**)	2.114 (**7**)
		2.141 (**8**)	2.145 (**3**)
	CH_3O	2.052 (**3**)	2.051 (**8**)
		2.044 (**4**)	2.034 (**9**)
	H_2CO	2.085 (**6**)	2.081 (**11**)
Ru–C	H_2CO	2.150 (**6**)	2.131 (**11**)
Ru–H	H	1.600 (**11**)	1.612 (**6**)

Table IV. Ru–Cl and Ru–P Bond Distances (Å) as a Function of Trans Ligands in Various Intermediates

	bond distance	
trans ligand	Ru–Cl	Ru–P
vacant[a]	2.344 (**4**)	2.305 (**9**)
η^2-OAc	2.362 (**1**)	2.339 (**1**)
CH_3OH	2.367 (**3**)	2.340 (**8**)
	2.367 (**7**)	2.352 (**2**)
H_2CO	2.369 (**11**)	2.347 (**6**)
η^1-OAc	2.371 (**2**)	2.356 (**7**)
CH_3O	2.392 (**8**)	2.367 (**4**)
	2.358 (**9**)	2.368 (**3**)
H	2.385 (**6**)	2.416 (**11**)

[a] In **4** the trans ligand is the agostic CH bond.

stereochemistry of $RuCl(H)(CO)(PEtPh_2)_3$ is well interpreted by the mechanism that deactivation takes place along path Cl and that, on the other hand, the formaldehyde ligand leaves the coordinating site intact along path P, with the catalytic cycle completed.

Our calculated results with respect to the two possible reaction paths are summarized as follows. (1) The acetato Ru–O bond trans-disposed to the phosphine ligand is weaker than the other in $Ru(\eta^2\text{-}OAc)Cl(PH_3)_3$. (2) $Ru(\eta^1\text{-}OAc)Cl(MeOH)(PH_3)_3$ with the methanol ligand trans-disposed to phosphine is more stable than that with the methanol ligand trans-disposed to chlorine. (3) $RuCl(OCH_3)(MeOH)(PH_3)_3$ with the methoxy ligand trans-disposed to phosphine gave $RuCl(OCH_3)(PH_3)_3$ more easily by methanol dissociation than that with the methoxy ligand trans-disposed to chlorine.

Points 1 and 2 show that formation of $Ru(\eta^1\text{-}OAc)Cl(MeOH)(PH_3)_3$ in path P is easier than in path Cl in the first stage of the catalytic reaction. Since at the MP2 level the CH bond splitting is downhill, $RuCl(OCH_3)(PH_3)_3$ should resemble the transition state. Consequently, point 3 indicates that the activation barrier in path P is lower. These can be explained in terms of trans influence; the orders we found are H > CH_3O > η^1-OAc > H_2CO, CH_3OH > η^2-OAc, and PH_3 > Cl. Preference of path P to path Cl was well demonstrated by the easier formation of the η^1-OAc complex and the lower activation barrier.

Our experimental results on the reaction path have thus been well reproduced by these ab initio calculations. The molecular design of catalytic activity, selectivity, and deactivation is now attainable on the basis of detailed theoretical analysis on energy profiles.

Acknowledgment. All the calculations were carried out at the Computer Center, Institute for Molecular Science (IMS), through a joint study program.